Available online at www.sciencedirect.com
ScienceDirect
Journal of the European Ceramic Society 26 (2006) 3161–3171
www.elsevier.com/locate/jeurceramsoc

# Sintering, microstructural development, and electrical properties of gadolinia-doped ceria electrolyte with bismuth oxide as a sintering aid

Vanesa Gil *, Jesus Tartaj, Carlos Moure, Pedro Durán

*Instituto de Cerámica y Vidrio (CSIC), Campus de Cantoblanco, Kelsen, 5, 28049 Madrid, Spain*

Received 9 June 2005; received in revised form 30 August 2005; accepted 3 September 2005
Available online 27 October 2005

**Abstract**

A considerable reduction (≥250 °C) in the sintering temperature, enhancement of the sintering density, and a slight improvement of the electrical properties, can be achieved by using bismuth oxide in the range of 0.2 to 2 wt.%, as a sintering aid for gadolinia-doped ceria (GDC) ceramic electrolytes. Dilatometric experiment (CHR) and SEM observations indicate that a liquid phase-assisting sintering mechanism contributes to the improvement in sintering density for bismuth oxide concentrations exceeding 0.5 wt.%. The addition of small amount of $Bi_2O_3$ ≤0.5 wt.% also results in the achievement of highly dense ceramic bodies (≥99% of theoretical density) after sintering at 1200 °C for 4 h, which indicates that the addition of $Bi_2O_3$ to gadolinia-doped ceria promoted the sintering process by a cooperating volume diffusion-liquid phase-assisting mechanism. Based on the lattice constant data, the solid solubility limit of $Bi_2O_3$ in gadolinia-ceria is, probably, lower than 1.0 wt.%. Grain size also increased with increasing $Bi_2O_3$ content up to 0.5 wt.% and then it decreased with further addition of $Bi_2O_3$. The addition of the smaller amounts of bismuth oxide, i.e., ≤1.0 wt.% $Bi_2O_3$ slightly enhanced the total ionic electrical conductivity of the gadolinia-doped ceria electrolyte. The sintering temperature strongly influenced the electrical conductivity of the doped-GDC ceramics. The best sample was that containing 1.0 wt.% $Bi_2O_3$ sintered at 1400 °C for 2 h which had an ionic electrical conductivity of 4 S $m^{-1}$ at 700 °C, and an activation energy of 0.58 eV for the oxide-ion conduction process in air.


*Keywords:* $CeO_2$–$Gd_2O_3$; Sintering; Microstructure; Electrical properties

## 1. Introduction

$CeO_2$-based materials have been widely studied as catalyst supports and promoters for heterogeneous catalytic reactions. On the other hand, they are an upcoming alternative solid electrolyte to yttria-stabilized zirconia (YSZ) in solid oxide fuel cell (SOFC) applications.[1–3] They have higher ionic conductivity and lower interfacial losses than YSZ, and can also operate at lower temperatures (500–700 °C). However, the preparation of ultrafine powders to be used as precursors for the manufacturing of dense bulk ceramics has become necessary and, in that sense, many synthesis approaches using wet chemistry have been used to improve the homogeneity and the sinterability of the so-obtained powders. In spite of this, such powders were usually fired to only 95% dense at fairly high temperatures (≥1550 °C), which implies a high energy cost precluding, thus, the possibility of cofiring this electrolyte with other SOFC components due to the solid-state reaction and interdiffusion between them at those sintering temperatures. It seems that a competitive sintering temperature should be ≤1400 °C for gadolinia-doped ceria, in which the mobility of $Ce^{4+}$ cations is reasonably low. Hence, methods to produce high-density gadolinia-doped ceria ceramics at reduced sintering temperatures are needed to obtain high-performanced materials. Several procedures have been used including the use of a general method based on the oxalate coprecipitation route to produce Gd, Sm, Y-$CeO_2$ sinterable powders, which sintered at temperatures as low as 1300–1350 °C with ≥97% dense materials.[4–6] With these parameters at hand, the choice of electrode and interconnector materials would be much easier and cheaper. At the operating conditions of the intermediate temperature SOFCs, a limit in both the temperature and oxygen-partial pressure still restricts its use. However, several

* Corresponding author. Tel.: +34 91 735 58 40; fax: +34 91 735 58 43.
*E-mail address:* vanesa@icv.csic.es (V. Gil).

0955-2219/$ – see front matter © 2005 Elsevier Ltd. All rights reserved.
doi:10.1016/j.jeurceramsoc.2005.09.068

experiments have shown that doped-ceria can work as an oxide-ion conductor electrolyte at temperatures well-below 700 °C and oxygen partial pressure $\geq 10^{-5}$ atm. Above those limits an oxygen loss can occur with the reduction of $Ce^{4+}$ to $Ce^{3+}$, and the corresponding appearance of electronic conduction along with the oxide-ion conduction.

$Ce_{0.9}Gd_{0.1}O_{1.95}$ dense ceramic membranes are needed for electrolytes but it is well known, as mentioned before, that ceria-based materials are very difficult to densify below 1500 °C by the conventional ceramic techniques when using mixed oxides as raw materials. Then the use of non-conventional methods or, as another alternative, using sintering aids to reduce the sintering temperature become necessaries. In this paper we report, at our best knowledge for the first time, the preparation of dense (≥98% of theoretical density) $Ce_{0.9}Gd_{0.1}O_{1.95}$ materials at 1200 °C for 4 h, starting from a commercial submicronized powders by using bismuth oxide as a sintering aid. The effect of $Bi_2O_3$ additions on the grain-growth process as well as on the electrical conductivity of these dense ceramics will also be reported.

## 2. Experimental procedure

Commercial gadolinia-doped ceria $CeO_2$–$Gd_2O_3$ powders (denoted Cerium-Gadolinium oxide 90–10 LSA, Rhodia GmbH, FRG) with an average crystallite size of 0.38 μm and specific surface of 12.4 $m^2\,g^{-1}$, were used as starting raw material. This is referred to as GDC powder hereafter. The total amount of impurities (mainly silica) was, according to the suppliers, less than 13 ppm. The dopant, in the 0.2–2.0 wt.% $Bi_2O_3$ concentration range, as bismuth nitrate ($Bi(NO_3)_3{\cdot}5H_2O$) dissolved in ethanol, was added to a GDC powder/ethanol suspension by stirring. After drying at 120 °C for 2 h, the powders were calcined at 700 °C for 2 h, granulated and isopressed at 200 MPa. After compaction, the green density of powder compacts was in the order of 50% of the theoretical density. Non-isothermal sintering was performed at a constant heating rate (CHR) of 2 °C/min up to 1600 °C in a dilatometer Netzsch (model 407/E of Geratebau, Selb.Bayern, Germany). The samples were also isothermally sintered at 1400 °C which was held for times from 0 to 8 h. The density of the samples after sintering was measured by the Archimedes method.

In order to study the possible influence of the $Bi_2O_3$ additive on the crystalline structure of the prepared samples, these were heat-treated at 1200–1400 °C for 2 h, milled in an agate mortar, and then characterized by X-ray diffraction (XRD) with a diffractometer Siemens (model D-5000, Erlangen, Germany) using nickel-filtered Cu Kα radiation (λ = 0.15405 nm). An internal alumina standard was used for the lattice parameter measurements. Besides this, a powder mixture containing GDC and $Bi_2O_3$ 50/50 in wt.% was homogeneized and heat-treated for several hours at 850–1000 °C for 2 h. The new-formed phases, if any, were also investigated by XRD.

The microstructure of the sintered samples was examined in a Zeiss (SEM) scanning electron microscope (model DSM 950, Oberkochem, Germany). The average grain size was measured by the line intercept method on the surface of polished and thermally etched sintered samples. The size of at least 300 grains was taken into account.

The electrical conductivity of the dense undoped and $Bi_2O_3$-doped GDC-sintered samples was measured by using a.c. impedance spectroscopy. Silver paint was backed onto each side of the sintered samples at 750 °C for 1 h, to ensure good contact with the samples. Platinum wires attached to the electrode provided current contacts to each electrode on the sintered samples. Impedance spectra were obtained using an LF Impedance Analyser (model 4192A, Hewlett-Packard) over the frequency range of 10 Hz–10 MHz. Measurements were made in the temperature range 150–500 °C in air. Grain interior (GI), grain boundary (GB), and electrode polarization contributions to the total electrical conductivity can be clearly identified within that temperature range, and the quantitative change in GI and GB conductivities were measured by fitting these impedance plots using the Equivalent Circuit Program. The total electrical conductivity was also measured in the temperature range of 150–700 °C at a fixed frequency of 10 kHz.

## 3. Experimental results

### 3.1. X-ray diffraction study

X-ray diffraction patterns of GDC powders without and with 0.2–2.0 wt.% $Bi_2O_3$ added after heat-treatment at 1200–1400 °C for 2 h (not shown here), revealed no free $Bi_2O_3$ or secondary peaks phase. If some secondary phase was formed the amount was too small to be detected by X-ray diffraction. The XRD peaks due to the fluorite solid solution of the GDC sample were slightly shifted to smaller angles with increasing $Bi_2O_3$ content, as shown in Fig. 1. The shifts were shown to increase with increasing $Bi_2O_3$ content up to 1 wt.% and then remained constant for higher additive concentration. The lattice constants were calculated from the higher angle lines in XRD patterns as a function of the additive content, as shown in Fig. 2. As can be seen, the lattice parameter increases linearly with increasing $Bi_2O_3$ up to about 0.8 wt.%, remaining constant for higher

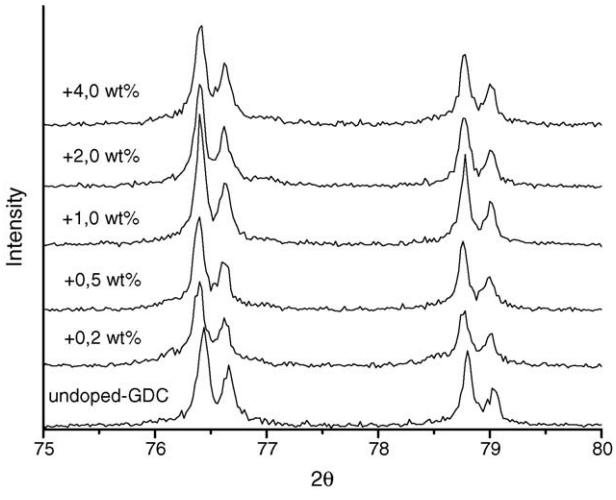


Fig. 1. High-angle X-ray diffraction patterns of doped-GDC samples sintered at 1400 °C for 2 h with different $Bi_2O_3$ contents.

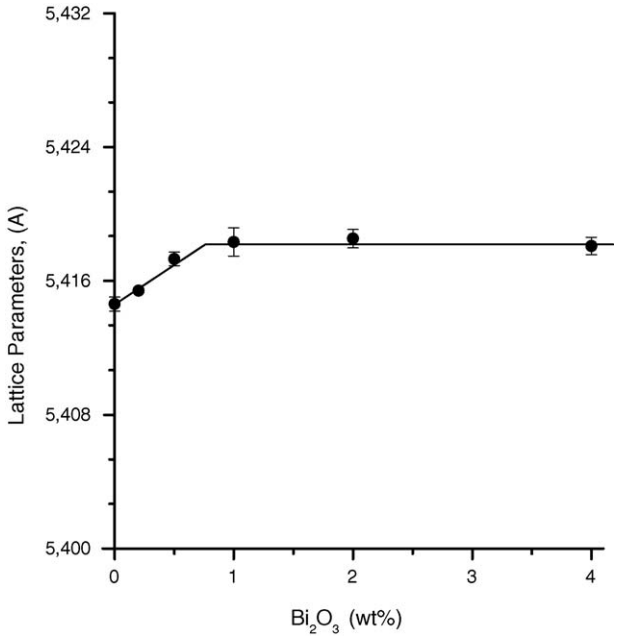


Fig. 2. Lattice parameters of the doped-GDC samples as a function of the $Bi_2O_3$ content.

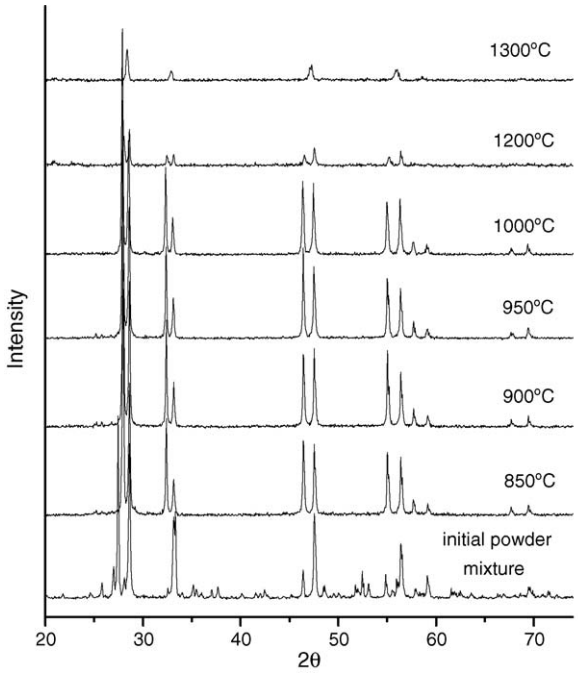


Fig. 3. XRD patterns of the GDC/$Bi_2O_3$ 50/50 wt.% powder mixture as a function of the temperature.

$Bi_2O_3$ concentrations. Such an increase will be probably due to the substitution of larger $Bi^{3+}$ ions ($r = 0.117$ nm) for $Ce^{4+}$ ions ($r = 0.097$ nm) in the cubic lattice of the GDC structure.[7] Hence, the solubility limit of $Bi_2O_3$ in gadolinia-doped ceria was estimated to be $\leq$0.8 wt.%. According to our experimental results, the $Bi_2O_3$ solubility does not change significantly over the 1200–1400 °C temperature range.

As is well known, the solubility range for dopants such as alkaline earth oxide or rare earth oxide in $CeO_2$ is very large.[8] However, given that the ionic radius of $Bi^{3+}$ is larger than that of $Ce^{4+}$, its dissolution in a gagolinia-doped ceria system will be limited.[9] Although a few reports are available on the solid solubility of sintering additives in solid electrolytes, mainly performed on the dissolution of $Al_2O_3$ and $Fe_2O_3$ in zirconia,[10] it is not the case of ceria-based electrolytes on which recently it has been the objective of several papers.[11–13] For example, the influence of some additives as Cu, Co, Ni, and Fe oxides on the sintering and electrical performances of both pure and doped-ceria have been carried out. But in no case was studied the effect of $Bi_2O_3$ as an additive for the sintering and electrical properties of ceria-based materials.

In order to better know the true effect of the $Bi_2O_3$ additions on the sintering behavior and electrical properties of GDC samples, a powder mixture GDC + $Bi_2O_3$ containing 50/50 in wt.% and heat-treated at 850–1000 °C for 2 h was studied. Fig. 3 shows the XRD patterns of the samples after the heat treatments. The objective of this specific task was to know more clearly the interaction, if any, between the bismuth oxide additive and the GDC electrolyte. As can be seen, the bismuth oxide reacts with the GDC electrolyte to give a cubic δ-$Bi_2O_3$–$Gd_2O_3$ phase yielding a GDC sample with a $Gd_2O_3$ concentration lower than in the original GDC ceramic. It allowed us to assume that the lattice constant of the new GDC sample will also be a little lower than that of the initial GDC raw material composition. Therefore, from the results of the XRD study and lattice parameter measurements, we can suggest that at low temperature, i.e., <1000 °C the small amounts of the added $Bi_2O_3$ firstly reacts with the $Gd_2O_3$ of the GDC sample to give the corresponding amount of a binary $Bi_2O_3$–$Gd_2O_3$ cubic solid solution with the structure of the δ-phase stabilized, probably, with a small amount of $CeO_2$. At temperatures higher than about 1000 °C such a binary solid solution is not more stable and decomposes, a part of the $Bi_2O_3$ enter into the GDC structure forming a ternary $CeO_2$–$Gd_2O_3$–$Bi_2O_3$ solid solution. The part of $Bi_2O_3$ exceeding 0.8 wt.% will assist the sintering process as a liquid phase at higher temperatures or, on the other hand, it can slowly evaporate thoroughly the sintering process.

### 3.2. Sintering behavior

Dilatometric measurements up to 1600 °C were made to study the sintering behavior of the undoped and $Bi_2O_3$-doped GDC samples. The results are shown in Fig. 4a and b. The shrinkage rate spectra of samples with several concentrations of $Bi_2O_3$ are shown in Fig. 4a. For comparison, the spectrum corresponding to that of the undoped-GDC samples is also included. The sintering process of the undoped-GDC samples takes place with the appearance of two shrinkage rate maxima, a small one at about 1250 °C, and the second one with the higher shrinkage rate at about 1520 °C. Between them an inflexion point at approximately 1400 °C occurred, i.e., the densification of the undoped-sample takes place in a two-stage process. When the $Bi_2O_3$ content is >0.5 wt.% only one pronounced peak appeared while the samples containing lower amounts of $Bi_2O_3$ $\leq$0.5 wt.% are somewhat broader, indicat-

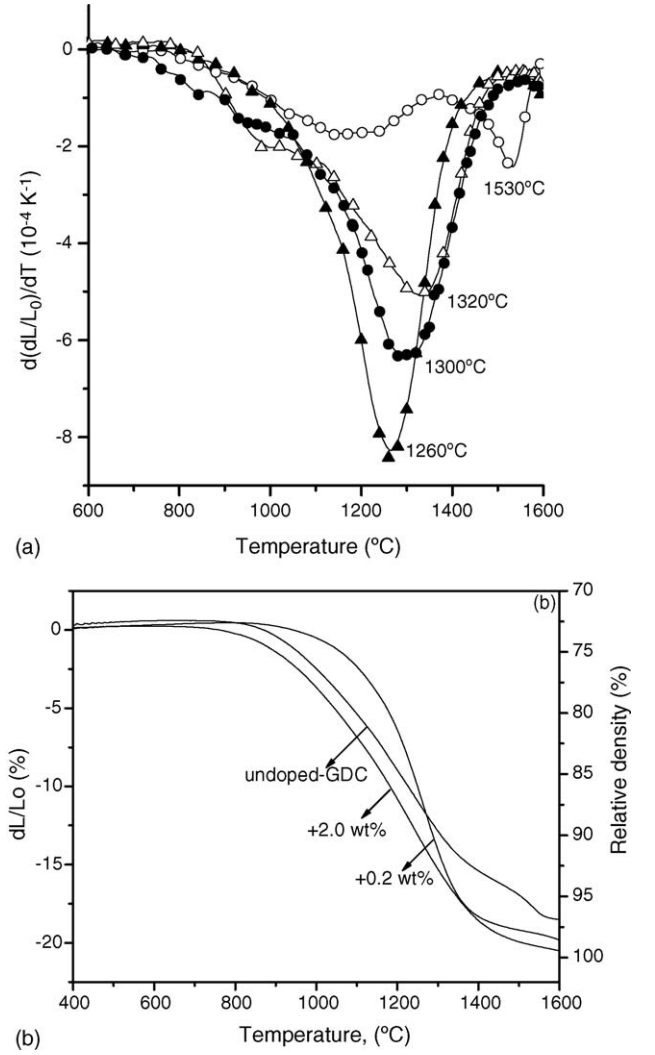


Fig. 4. (a) Linear shrinkage rate vs. sintering temperature (◯) undoped-GDC, (△) +0.5 wt.% $Bi_2O_3$, (●) +1.0 wt.%, and (▲) +2.0 wt.%. (b) Relative density vs. temperature for undoped and doped-GDC samples.

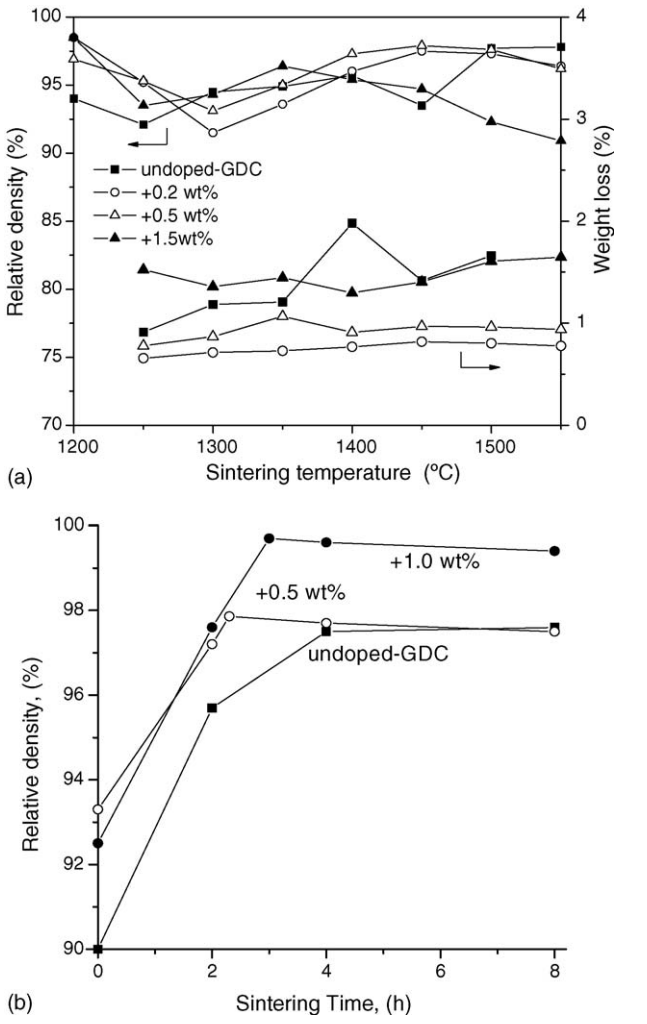


Fig. 5. (a) Relative density and weight loss as a function of the sintering temperature for 2 h and (b) relative density as function of the sintering time at 1400 °C.

ing a more gradual densification. For $Bi_2O_3$ contents >0.5 wt.% the temperature of the shrinkage rate maximum decreased up to 1250 °C with $Bi_2O_3$ increasing to 2.0 wt.%. From that figure it is clear that $Bi_2O_3$ additions does change the sintering mechanism of GDC samples. On the other hand, it can also be seen that the maximum shrinkage rate of doped-GDC samples are increased by a factor of 2–5 compared to undoped-GDC ones. Fig. 4b shows the linear shrinkage of the 0.2 and 2.0 wt.% $Bi_2O_3$-GDC samples as a function of the temperature comparatively with that of the undoped-GDC sample. It can be observed that the undoped-GDC sample do not reached its final shrinkage below 1600 °C with a shrinkage of about 18%, while the samples containing 0.2 wt.% $Bi_2O_3$ reached its final shrinkage at about 1450 °C and a shrinkage of 21%. From that figure it is also clear that the $T_s$, i.e., the temperature at which the relative density of the sintered sample attains 95% of theoretical density, decrease from about 1580 °C for the undoped-samples to 1370 °C, i.e., more than 200 °C with the only addition of 0.2 wt.% $Bi_2O_3$. It must be mentioned that all samples reached 96–99% of theoretical density at the end of the non-isothermal sintering process.

Fig. 5a and b shows the effect of $Bi_2O_3$ additions on the densification of GDC samples heat-treated at 1100–1600 °C for 2 h. The beneficial effect of the $Bi_2O_3$ additions on the sintering of the GDC samples is such that while the undoped-GDC ones reached sufficient density, i.e., 95% of theoretical, after they are sintered at a temperature as high as 1400–1500 °C for 2 h, the addition of only 0.2 wt.% $Bi_2O_3$ strongly enhances the densification rate such that the samples attained a density as high as 99.3% of theoretical after sintering at only 1100–1200 °C for 2 h, and still 97.5% dense for the composition containing 1.0 wt.% $Bi_2O_3$ at the same temperature. A dedensification phenomenon, i.e., a decrease in density with increasing temperature seems to take place in the doped-GDC samples for temperatures higher than 1200 °C, and such a decrease is a maximum at 1295, 1300, and 1350 °C for 0.2, 0.5, and 1.0 wt.% $Bi_2O_3$, respectively. The density of these samples increase again with further increasing temperature. In the same Fig. 5a the weight loss as a function of the temperature has also been represented and, as can be seen,

the maximum in dedensification coincides with the maximum in the weight loss curves, i.e., in the temperature range of 1300–1350 °C for the doped-GDC samples. As can be observed, the weight loss in all the doped-GDC samples was always higher than that corresponding to the $Bi_2O_3$ content. In the case of the undoped-GDC samples the density increases monotonically with increasing temperature up to 1400 °C, above which also a dedensification phenomenon is present with a density decreasing between 1400 and 1450 °C, and further increase in density again as the temperature was increased. As with the doped-GDC samples, the maximum in the density decrease coincided with the maximum in the weight loss of the undoped-GDC sample, which occurred within the same temperature range.

The effect of the $Bi_2O_3$ additions in enhancing the densification of GDC electrolytes was also evidenced by studying the evolution of the density of the samples as a function of the sintering time. As it is shown in Fig. 5b, the density of the undoped-GDC samples monotonically increases with increasing sintering time, reaching a density of 97.6% after sintering at 1400 °C for 8 h. However, the doped-GDC samples attain a density as high as 97.9 and 99.7% of theoretical density for shorter sintering time at the same sintering temperature. From these results we can suggest that the addition of small amounts of $Bi_2O_3$ to GDC electrolytes strongly enhances the sintering behavior of these ceramics, but its density decreased when the sintering temperatures are relatively high (≥ 1350–1400 °C) and/or the sintering time is too long (≥ 2–3 h).

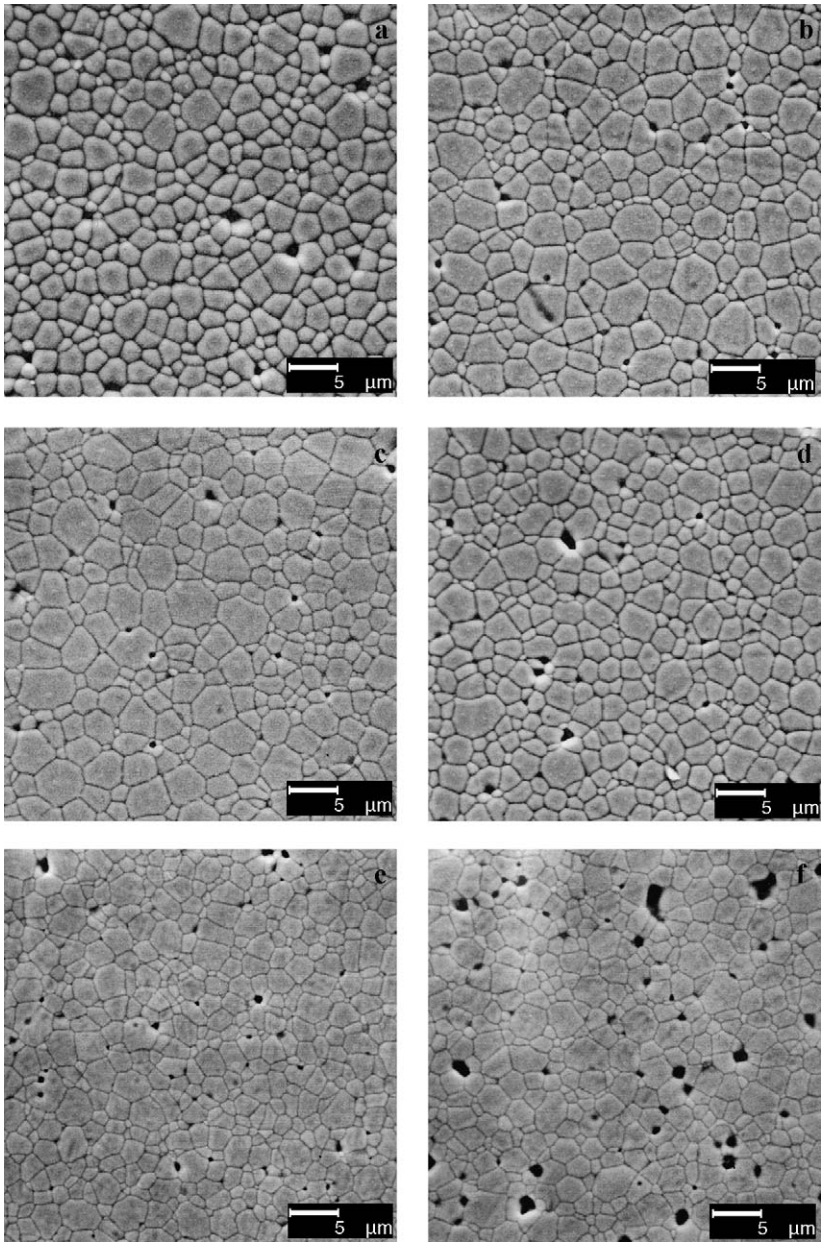


Fig. 6. Microstructures of the undoped-GDC (a) and 0.2–2 wt.% $Bi_2O_3$-doped GDC samples (b–f) sintered at 1600 °C without holding time.

### 3.3. Microstructural development

The influence of $Bi_2O_3$ additions on grain growth during sintering of GDC electrolyte is an important factor, besides a high density, to define its performances when this is used in a SOFC device. Fig. 6 shows the scanning electron micrographs of the polished and thermally etched surfaces for (a) the undoped-GDC samples, and (b–f) for $Bi_2O_3$-doped GDC samples after sintering at 1600 °C without holding time. From that figure it can be identified three well-defined regions for the average grain size as a function of the $Bi_2O_3$ concentration. A first region up to 0.5 wt.% $Bi_2O_3$, in which the average grain size slightly increases from 2.85 μm in the undoped-GDC sample Fig. 6a to 3.40 μm for the GDC sample containing 0.5 wt.% $Bi_2O_3$, Fig. 6c; a second region for samples containing between 1.0 and about 2.0 wt.% $Bi_2O_3$ in which the average grain size slightly decreases up to 2.85 μm with increasing $Bi_2O_3$ content, Fig. 6d–f. Above that $Bi_2O_3$ concentration, not shown here, a third region in which the sintered GDC samples showed a bimodal microstructure which consisted of relatively large grains (≥ 3.5 μm) accompanied by other smaller grains (≤0.5 μm) within or in the boundary of the larger grains. Fig. 7 shows the variation of the average grain size of the doped-GDC samples with the $Bi_2O_3$ content at 1600 °C in the non-isothermal sintering conditions, and at 1400 and 1200 °C for 2 h, respectively. At 1600 °C, i.e., in the final-stage of sintering, it seems to be that the smaller $Bi_2O_3$ additions substantially promote the grain growth kinetics of the GDC samples, whereas further addition of $Bi_2O_3$ do not make it, i.e., the GDC grain size is dependent on the $Bi_2O_3$ content to about 0.5 wt.%, and this dependence decreases with further additions of $Bi_2O_3$ to 2.0 wt.%. At the intermediate-stage of sintering, i.e., at 1400 °C, the $Bi_2O_3$ additions does not appear to significantly affect the grain size of the doped-GDC samples, rather it inhibited the grain growth kinetics and the grain size remained almost constant or slightly decreased. At the earlier sintering stages, i.e., at or below 1200 °C, the grain size is not or hardly dependent on the $Bi_2O_3$ added.

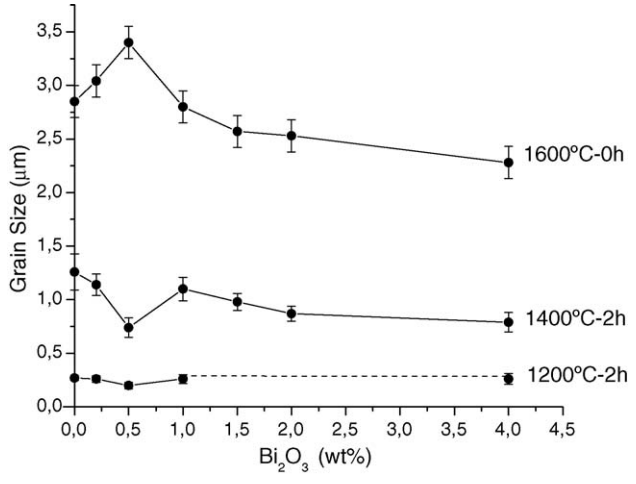


Fig. 7. Grain size as a function of the $Bi_2O_3$ content of doped-GDC samples at different sintering temperatures.

### 3.4. Electrical properties

Firstly, to better know the real effect of the $Bi_2O_3$ additions on the electrical response of the doped-GDC samples, the electrical measurements were carried out on those sintered at 1400 °C for 2 h, i.e., with a sufficiently high relative density (≥95% of theoretical) and with a well-developed microstructure. Fig. 8a shows, as a representative example, the impedance plots for the $Bi_2O_3$-doped GDC samples containing 1.0 wt.% $Bi_2O_3$ measured at different temperatures in the range of 150–500 °C. Given that the doped-GDC samples containing 1.5 and 2.0 wt.% $Bi_2O_3$ also have a quite similar impedance characteristics, the impedance spectra of those samples have not been included in Fig. 8a for clarity. Two well-separated arcs and portions of a third at the lower frequencies were observed for all samples. Similar results were found and both the grain interior (GI) and the grain boundary (GB) contributions well established before for yttria-stabilized zirconia.[14] The grain-interior or bulk conductivity, $\sigma_{GI}$, is then calculated taken into account the bulk resistance $R$ according to the relation, $\sigma_{GI} = (1/R) \times (L/S)$, where $L$ and $S$ are the geometrical dimensions of the sample. In the same way the grain-boundary conductivity, $\sigma_{GB}$, can also be calculated. Fig. 8b shows the evolution of the impedance arcs as a function of the $Bi_2O_3$ concentration at a fixed temperature compared to that of the undoped-GDC samples. As it could be expected from that figure, the arc corresponding to the grain-interior contribution, for a given temperature, should remain nearly identical for all samples and this did not occur in the present case, i.e., it surprisingly vary from sample to sample, showing a monotonically impedance decrease up to 1.0 wt.% $Bi_2O_3$ and then again increased. Such slight GI impedance decrease can be strongly related with the dissolution of some $Bi_2O_3$ into the cubic lattice of the GDC structure. However, the arc corresponding to the grain-boundary, i.e., at the lower frequencies, as expected, clearly change for each sample. It is found that the GB impedance also decreases as the $Bi_2O_3$ increases from 0.2 to 1.0 wt.% for which the GB impedance is quite similar to that of the undoped-GDC samples. Beyond such a $Bi_2O_3$ concentration, both the GI and the GB contribution seem to affect negatively to the total conductivity of the doped-GDC samples. Such a particular behavior of the doped-GDC samples will be explained later on. The best electrical conductivity ($\sigma_t = 1.25 \times 10^{-1}$ S/m at 340 °C) was found for the doped-GDC samples containing 1 wt.% $Bi_2O_3$, which is slightly higher than that of the undoped-GDC samples ($\sigma_t = 8.5 \times 10^{-2}$ S/m) measured at the same temperature. In the same way, the $\sigma_{GI}$ and $\sigma_{GB}$ conductivities were a factor of 1.5 higher than that for undoped-GDC samples. However, the total conductivity of both kind of samples measured at a fixed frequency of 10 kHz in the temperature range of 200–700 °C was very similar, i.e., 4.1 against 4.0 S/m for undoped and 1.0 wt.% $Bi_2O_3$-doped GDC samples, respectively. This result indicates that the grain boundary conductivity dominates the conduction process.

Secondly, since the physical and chemical nature of the $Bi_2O_3$ additive is different along the sintering process, electrical measurements also were carried out on the undoped and 1.0 wt.% $Bi_2O_3$-doped GDC samples sintered at 1200 °C for 2 h. It is

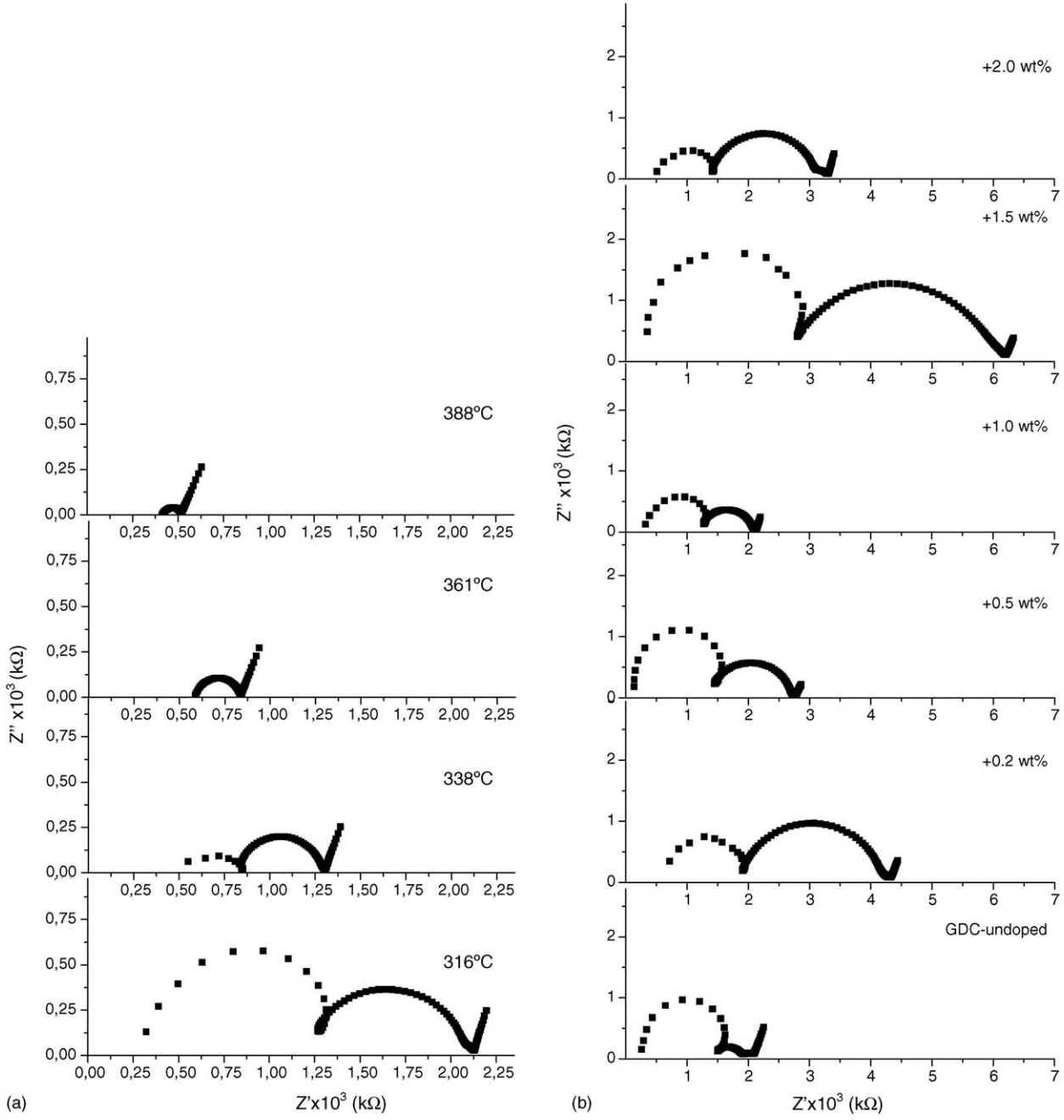


Fig. 8. Impedance spectra of GDC samples doped with 1 wt.% $Bi_2O_3$ as a function of the temperature (a), and impedance spectra of GDC samples as a function of the $Bi_2O_3$ content at 315 °C.

noticeable that the addition of 1.0 wt.% $Bi_2O_3$ lead to a slight decrease in $\sigma_{GI}$, $\sigma_{GB}$, and $\sigma_t$ conductivities, and these were a factor of about 1.5 lower than that of undoped-GDC samples in $\sigma_{GI}$ and $\sigma_t$, but the $\sigma_{GB}$ decreased about 3.2 times that of the undoped-GDC samples. From all the above, it can be suggested that the electrical properties of doped-GDC samples are strongly influenced by the sintering temperature.

Fig. 9 shows the Arrhenius plots of the grain interior, the grain-boundary, and total conductivities of the doped-GDC samples containing 1.0 wt.% $Bi_2O_3$. The activation energies were calculated from the $\log \sigma$ versus $1/T$ plots in the temperature range of 150–500 °C and these are shown in Table 1. When the Arrhenius plots for the data of the total conductivity obtained in the temperature range of 200–700 °C at a constant frequency were represented, not shown here, it was found that the activation energy hardly varied in all the $Bi_2O_3$ concentration range, being this of 0.57 eV for the undoped-GDC samples and of 0.56 eV for that containing 2.0 wt.% $Bi_2O_3$. As the more important fact, Fig. 10 shows, comparatively, the Arrhenius plots for the undoped-GDC and doped-GDC samples containing 1.0 wt.% $Bi_2O_3$ sintered at 1200 and 1400 °C for 2 h, respectively. These results evidenced again the strong influence of the sintering temperature on the electrical properties of the GDC ceramics. As mentioned above, Table 1 summarizes the main characteristics

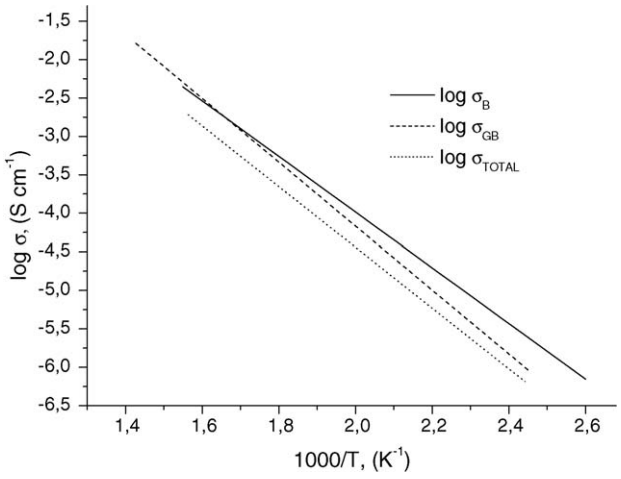


Fig. 9. Arrhenius plots of $\sigma_{GI}$, $\sigma_{GB}$, and $\sigma_t$ electrical conductivities in air for GDC samples with 1 wt.% $Bi_2O_3$.

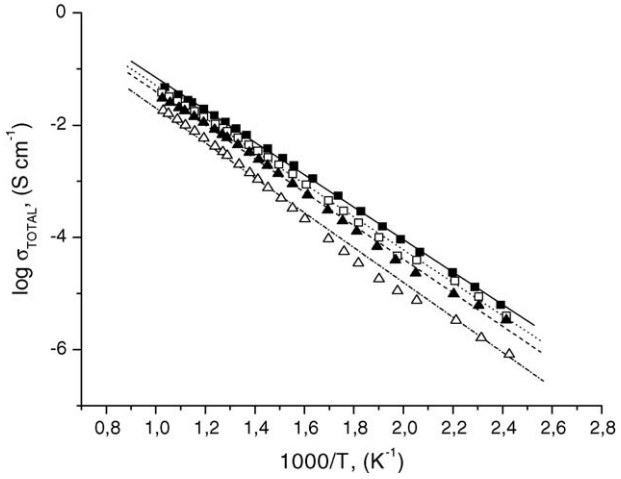


Fig. 10. Arrhenius plots of the $\sigma_t$ for undoped and 1 wt.% $Bi_2O_3$-doped GDC samples sintered at 1200 and 1400 °C for 2 h.

for both the undoped and 1.0 wt.% $Bi_2O_3$-doped GDC-sintered samples.

## 4. Discussion

From the above experimental results in Figs. 4 and 5, it can be suggested that the addition of small amounts of $Bi_2O_3$ (0.2–2.0 wt.%) completely changes the sintering mechanism, enhancing the densification rate and reducing the sintering temperature of gadolinia-doped ceria ceramics. Several factors have to be considered to reasonably well explain such a sintering behavior. The global non-isothermal sintering process of the doped-GDC samples, depending on both the $Bi_2O_3$ content and the temperature, can be divided in three main regions,

(i) A first region up to 1200 °C (≈83% of relative density, i.e., with still open and interconnected porosity) in which the main features on the densification process seems to take place. For the lower $Bi_2O_3$ concentration (0.2 and 0.5 wt.%) and, if it is assumed that for undoped-GDC sintering is dominated by solid-state diffusion,[15,16] then we can also assume that at this region an insufficient amount of liquid phase to wet all the grain boundaries occurred and, therefore, it can be stated that a transition between volume diffusion and viscous flow mechanisms take place. In such a way, a cooperative contribution of both with a rapid rearrangement of the solid GDC particles in the formed liquid phase diminishing the inter-particle friction and enhancing so the densification rate, as shown in Fig. 4a, can be assumed to dominate the densification process within this $Bi_2O_3$ concentration range. A similar argument for the sintering mechanism in the case of the pure $CeO_2$ containing an amount of $Fe_2O_3$ lower than 0.5 wt.% was reported.[12,17] For $Bi_2O_3$ contents ≥ 1.0 wt.% the densification rate is extremely increased in such a way that the temperature necessary to achieve the same density level, for example 95% of theoretical, is about 1300 °C in the GDC samples containing 2.0 wt.% $Bi_2O_3$, while that is of 1520 °C in the case of the undoped-GDC samples, i.e.,

Table 1
Main characteristics of undoped and 1 wt.% $Bi_2O_3$-doped GDC ceramics

| Composition | $T_s$ (°C) | Density (%) | Grain size (μm) | $\sigma_{GB\ (340°C)}$ (S/m) | $\sigma_{GI\ (340°C)}$ (S/m) | $\sigma_{T\ (340°C)}$ (S/m) | $\sigma_{T\ (700°C)}$ (S/m) | $E_{GB}$ (eV) | $E_{GI}$ (eV) | $E_T$ (eV) | $E_{T\ (700°C)}$ (eV) |
|---|---|---|---|---|---|---|---|---|---|---|---|
| Undoped-GDC + 1 wt.% $Bi_2O_3$ | 1200 (2 h) | 93.5<br>97.7 | 0.36<br>0.33 | $8.5 \times 10^{-2}$<br>$2.46 \times 10^{-2}$ | $1.60 \times 10^{-1}$<br>$7.21 \times 10^{-2}$ | $4.03 \times 10^{-2}$<br>$2.07 \times 10^{-2}$ | 2.7<br>1.8 | 0.80<br>0.84 | 0.70<br>0.66 | 0.76<br>0.80 | 0.59<br>0.68 |
| Undoped-GDC + 1 wt.% $Bi_2O_3$ | 1400 (2 h) | 95.6<br>97.5 | 1.26<br>1.10 | $2.15 \times 10^{-1}$<br>$2.35 \times 10^{-1}$ | $1.25 \times 10^{-1}$<br>$2.66 \times 10^{-1}$ | $0.87 \times 10^{-1}$<br>$1.25 \times 10^{-1}$ | 4.1<br>4.0 | 0.83<br>0.82 | 0.67<br>0.71 | 0.78<br>0.77 | 0.57<br>0.58 |
| 0.5 at.% Fe-GDC[32,a] | 1450 (5 h) | 98 | >10 | $5.91 \times 10^{-2}$ | $3.93 \times 10^{-2}$ | – | 6.17 | 1.01 | 0.88 | 0.89 | – |
| 30 ppm $SiO_2$-GDC[27] | 1600 (5 h) | 96.5 | 2.3 | $2.0 \times 10^{-1}$ | $4.14 \times 10^{-2}$ | – | 1.65 | 0.92 | 0.768 | 0.826 | – |

[a] The data of $\sigma_T$ for the references 27 and 32 were measured at 600 and 750 °C, respectively.

more than 200 °C lower, see Fig. 4b. Also at a concentration of $Bi_2O_3$ ≥1.0 wt.%, the sudden increase in shrinkage rate as observed for $Bi_2O_3$ = 2 wt.% in Fig. 4a, i.e., in the presence of a sufficient amount of liquid phase, the densification process can be considered as taking place by a liquid phase-assisted mechanism.[9,10] Furthermore, at this first region which we can consider as to be associated to the early-stage sintering,[17] the grain size is hardly affected by the presence of the additive, see Fig. 7. To support such a suggestion, it can also be assumed that at or below 1200 °C, the viscosity and surface tension of the formed liquid are too high impeding, thus, the diffusion of some material. Being this so, then our suggestions would be in close agreement with the suggestions of Cameron et al.[18] and Nadaud et al.[19] who reported that the grain size remained unchanged for relative density values lower than about 90%, i.e., when the porosity changed from being open and interconnected to closed. It must also be noted that all the above suggestions for this first region are based on the assumption that the $Bi_2O_3$ amount present in the doped-GDC samples is close or near to the nominal composition, i.e., the weight loss due to a partial evaporation of $Bi_2O_3$, as shown in Fig. 5a, is very small or practically null.[20]

(ii) A second region, above 1000–1200 °C and up to about 1350–1400 °C (≈95% of relative density, i.e., with closed porosity), in which the densification rate in doped-GDC samples is controlled by the presence of a transient bismuth-rich liquid phase, the release of oxygen gas (from some reduction of $CeO_2$ to $Ce_2O_3$), and the volatilization of $Bi_2O_3$ with increasing temperature. This suggestion is in close agreement with that reported in the literature,[21] in which a temperature above 1100 °C is considered as reasonable for the beginning of the $Bi_2O_3$ evaporation. On the other hand, it must be taken into account that, as mentioned before, the weight loss always was higher than that corresponding to the $Bi_2O_3$ content, which supported the idea that some oxygen gas is also lost along with $Bi_2O_3$. At that temperature interval, porosity is generated mainly as consequence of the $Bi_2O_3$ volatilization and the evolution of the density, as is shown in Fig. 5a, is controlled by the amount of $Bi_2O_3$ evaporated. The density slightly decreases and reached a minimum at 1350 °C in which we have considered that the majority of the $Bi_2O_3$, but not all, has been eliminated from the doped-GDC samples, i.e., at this temperature range the viscosity and surface tension will be much lower than that at 1200 °C, but the generated new porosity has a pinning effect on the grain boundaries mobility and very little grain growth took place at or below 1400 °C, see Fig. 7. This second region, with a slow grain growth but with a homogeneous grain size, in which the doped-GDC samples are sufficiently dense (≥95% theoretical) and microstructurally tougher than those samples processed within the first region, we associates with the intermediate-stage sintering. In this way, it can be considered 1350–1400 °C as a competitive temperature for the preparation of these doped-GDC ceramics and its application in a co-sintering process.

(iii) Above 1400 °C, a third region seems to exist in which a similar dedensification phenomenon in the undoped-GDC samples occurred. The density of these samples rapidly decreased to a minimum (below 93% of theoretical) at a temperature of 1450 °C. We remember here that such a temperature coincides with that of the inflection point mentioned in the shrinkage rate curve of these samples, see Fig. 4a. The cause for such a dedensification can be attributed to a weight loss as a consequence of the reduction of $Ce^{4+}$ to $Ce^{3+}$ with the production of oxygen gas. Such a suggestion is in close agreement with that reported on the sintering at high temperature (>1300 °C) of nanosized $CeO_2$ powders,[22] and by those of Boutz et al.[23] and Theunissen et al.[24] who found that the reduction of $Ce^{4+}$ to $Ce^{3+}$ in ceria during sintering in air takes place at 1150–1400 °C in yttria-ceria-stabilized tetragonal zirconia polycrystals. A similar phenomenon also was reported for the sintering of $LaFeO_3$ perovskite.[25] Such a third region, dominated by the closure of the pores along with a rapid grain growth by the solid-state reaction mechanism correspond, according to the suggestions of Kingery et al.,[26] to the well known as final-stage sintering. In the case of the doped-GDC samples, it seem to be that a kinetic competition between the closure rate of pores and the weight loss due to both the volatilization of some residual $Bi_2O_3$ still remaining in the samples and the evolution of oxygen gas, is to be present at this last-stage sintering.

It is widely accepted that the electrical behavior of a zirconia-based electrolyte is mainly determined by the grain-boundary electrical contribution which, at least in those contaminated with a relatively high level of $SiO_2$, dominates the total electrical conductivity.[27,28] Therefore, it is crucial to control the grain boundary nature and how to act on the same to enhance the final electrical performances of the electrolyte during service. In the case of the ceria-based electrolyte only a few papers have contributed to better know their electrical performances when installed in a SOFC device.[29,30] In this sense, we suggest that the addition of small amounts of $Bi_2O_3$ (≤1.0 wt.%) can improve the $\sigma_{GB}$, $\sigma_{GI}$, and $\sigma_t$ conductivities in such a way that, as shown in Table 1 for samples sintered at 1400 °C, the total conductivity is increased in a factor of almost two when the addition was of 1.0 wt.% $Bi_2O_3$. Although the influence of this additive is not very remarkable on the improvement of the GB conductivity, but the GI conductivity is significantly enhanced. Our microstructural studies revealed that when the amount of liquid phase is sufficient, i.e., for $Bi_2O_3$ concentrations ≥1.0 wt.%, the additive beneficially acts to remove mainly Si, also other impurities, from the grains during sintering maintaining them as such in the three-grain junctions, i.e., the additive can be playing a role of scavenger in the doped-GDC ceramics. The no evidence for a continuous thin liquid film at grain boundaries, at least by SEM observations, favored the oxygen ion mobility through both the interior of the grain and the grain-to-grain contacts. As it can be seen in Table 1, the effect of 1.0 wt.% $Bi_2O_3$ in enhancing $\sigma_{GB}$, $\sigma_{GI}$, and total conductivities was almost one order of magnitude higher than that achieved with the $Fe_2O_3$ addition.

As it has been experimentally established (see Figs. 9 and 10), the total electrical conductivity for the doped-GDC samples sintered at 1200 °C was much lower than that of the undoped-GDC samples. Such a behavior suggested us some comments: for example, as we have to assume that no phase transformation is to be present in ceria-based electrolytes then, in agreement to the results of Fig. 3, we must also expect that at this temperature $Bi_2O_3$ firstly reacts with the equivalent amount of $Gd_2O_3$ and $CeO_2$ to form the stabilized $Bi_2O_3$–$Gd_2O_3$ cubic δ-phase[31] which, on increasing temperature, melts and/or decomposes above 900 °C to give a complex liquid phase located at grain boundaries, and the specific resistivity of such a liquid phase has to be sufficiently high as to dominate the conduction process. The much lower grain boundary conductivity, $\sigma_{GB}$, measured at this temperature on the 1.0 wt.% $Bi_2O_3$-doped GDC samples (see Table 1) supported such a suggestion. To better know the electrical behavior of $Bi_2O_3$-doped GDC ceramics a deeper study of some parameters such as the optimum sintering temperature, microstructure, grain size and samples annealing become necessary. Such a research work is now in progress.

## 5. Conclusions

Additions of 0.2–2.0 wt.% $Bi_2O_3$ onto commercial GDC promoted densification rate, and theoretically dense bodies in the case of the doped-GDC containing 1.0 wt.% $Bi_2O_3$ after sintering at 1400 °C for 4 h, i.e., such a $Bi_2O_3$-doping reduces sintering temperatures over 200 °C. Further addition of $Bi_2O_3$ above 1 wt.% deteriorated density. The strongly enhanced densification rate in GDC samples was attributed to a fullness liquid phase-assisted sintering mechanism. The solubility limit of $Bi_2O_3$ in $Ce_{0.9}Gd_{0.1}O_{1.95}$ ceramics was estimated to be about 0.8 wt.% in samples sintered at 1200–1400 °C. Gadolinia-doped ceria samples with 1.0 wt.% $Bi_2O_3$ added sintered at 1400 °C had the same or smaller grain size of undoped-GDC, suggesting that $Bi_2O_3$ additions retarded or at least do not promotes grain growth up to or below 1400 °C.

Sintering temperature strongly affected the electrical behavior of the $Bi_2O_3$-doped GDC ceramics, and it was attributed to a scavenging effect of $Bi_2O_3$ giving rise to cleaner grain-to-grain contacts favoring the oxygen-vacancies mobility. At the temperature range of 200–700 °C, the total conductivity was as high as 4.0 S/m which is similar to that of the undoped-GDC samples (4.1 S/m). The slightly higher activation energy calculated for the oxide-ion conduction process in the doped-GDC samples, 0.58 eV, against 0.57 eV for the undoped-GDC ones support the suggestion of a higher grain boundary density in the doped-GDC ceramics, which detrimentally affect the total conductivity.

## Acknowledgements

The present work was financed by the CICYT under the Project CICYT, MAT 2003-0111163, and a grant from the Autonomus Community of Madrid.

## References

1. Steele, B. C. H., Appraisal of $Ce_{1-y}Gd_yO_{2-y/2}$ electrolytes for IT-SOFC operation at 500 °C. *Solid State Ionics*, 2000, **129**, 95–110.
2. Maricle, D. L., Swaar, T. E. and Karavolis, S., *Solid State Ionics*, 1992, **52**, 173–182.
3. Godikemeiker, M., Sasaki, K. and Gauckler, L. J., Electrochemical characteristics of cathodes in solid oxide fuel cells based on ceria electrolytes. *J. Electrochem. Soc.*, 1997, **144**, 1635–1646.
4. Duran, P., Moure, C. and Jurado, J. R., Sintering and microstructural development of ceria-gadolinia dispersed powders. *J. Mater. Sci.*, 1994, **29**, 1940–1948.
5. Van Herle, J., Horita, T., Sakai, N., Yokokawa, H. and Dokiya, M., Low-temperature fabrication of (Y, Gd, Sm)-doped ceria electrolyte. *Solid State Ionics*, 1996, **86–88**, 1255–1258.
6. Igashi, K., Sonoda, K., Ono, H. and Sameshima, M., Microstructure of rare-earth-doped ceria prepared by oxalate coprecipitation method. *J. Mater. Res.*, 1999, **14**, 957–961.
7. Shannon, R. D., Revised effective ionic radii in halides and chalcogenides. *Acta Crystallogr.*, 1976, **A32**, 751–767.
8. Chen, P. L. and Chen, I.-W., Grain growth in CeO2: dopant effects, defect mechanism, and solute drag. *J. Am. Ceram. Soc.*, 1996, **79**, 1793–1800.
9. Keizer, K., Burggraaf, A. J. and de With, G., The effect of $Bi_2O_3$ on the electrical and mechanical properties of $ZrO_2$–$Y_2O_3$ ceramics. *J. Mater. Sci.*, 1982, **17**, 1095–1102.
10. Verkerk, M. J., Winnubst, A. J. A. and Burggraaf, A. J., Effect of impurities on sintering and conductivity of yttria-stabilized zirconia. *J. Mater. Sci.*, 1982, **17**, 3113–3122.
11. Kleinlogel, C. and Gauckler, L. J., Sintering and properties of nanosized ceria solid solutions. *Solid State Ionics*, 2000, **135**, 567–573.
12. Kleinlogel, C. and Gauckler, L. J., Sintering of nanocrystalline $CeO_2$ ceramics. *Adv. Mater.*, 2001, **13**(14), 1081–1085.
13. Zhang, T., Hing, P., Huang, H. and Kilner, J., Sintering and grain growth of Co-doped $CeO_2$ ceramics. *J. Eur. Ceram. Soc.*, 2002, **22**, 27–34.
14. Aoki, M., Chiang, Y. M., Kosaki, I., Lee, L. J. R., Tuller, H. and Liu, Y., Solute segregation and grain-boundary impedance in high purity zirconia. *J. Am. Ceram. Soc.*, 1996, **79**, 1169–1180.
15. Zhang, T., Hing, P., Huang, H. and Kilner, J., Densification, microstructure and grain growth in the $CeO_2$–$Fe_2O_3$ system ($0 \leq Fe/Ce \leq 20\%$). *J. Eur. Ceram. Soc.*, 2001, **21**, 2221–2228.
16. Coble, R. L., Sintering crystalline solids: II. *J. Appl. Phys.*, 1961, **32**, 793–799.
17. Germann, R. M., *Liquid Phase Sintering*. ed. Plenum Press, New York, USA, 1985.
18. Cameron, C. P. and Raj, R., Grain growth transition during sintering of colloidally prepared alumina powder compacts. *J. Am. Ceram. Soc.*, 1988, **71**, 1031–1035.
19. Nadaud, N., Kim, D. and Boch, P., Titania as a sintering additive in indium oxide ceramics. *J. Am. Ceram. Soc.*, 1997, **80**, 1208–1212.
20. Drofenik, M., Znidarsic, A. and Markovec, D., Influence of the addition of $Bi_2O_3$ on the grain growth and magnetic permeability of MnZn ferrites. *J. Am. Ceram. Soc.*, 1998, **81**, 2841–2848.
21. Oeshev, P. and Pecheva, M., A study of sintering and magnetic parameters of spinel lithium ferrite, II. Lithium ferrite containing $Bi_2O_3$. *Mater. Res. Bull.*, 1980, **15**, 1199–1205.
22. Zhou, Y. and Rahaman, M. N., Effect of redox reaction on the sintering behavior of cerium dioxide. *Acta Mater.*, 1997, **45**, 3635–3639.
23. Bouth, M. M. R., Winnubst, A. J. A. and Burggraaf, A. J., Yttria-ceria stabilized TZP: sintering, grain growth and grain boundary segregation. *J. Eur. Ceram. Soc.*, 1994, **13**, 89–102.
24. Theunissen, G. S. A., Winnubst, A. J. A. and Burggraaf, A. J., Surface and grain boundary analyses of doped zirconia ceramics studied by AES and XPS. *J. Mater. Sci.*, 1992, **27**, 5057–5066.
25. Sagdahl, L. T., Einarsrud, M. A. and Grande, T., *J. Am. Ceram. Soc.*, 2000, **83**, 2318–2320.
26. Kingery, W. D., Bowen, H. K. and Uhlmann, D. R., *Introduction to Ceramics* (*2nd ed.*). Wiley, New York, 1976.

27. Zhang, T. S., Ma, J., Kong, L. B. and Chan, S. H., Effect of $SiO_2$ content on the ionic conductivity of $Ce_{0.8}Gd_{0.2}O_{2-\delta}$ ceramics. *J. Mater. Sci.*, 2004, **39**, 6371–6373.
28. Zhang, T. S., Ma, J., Chan, S. H. and Kilner, J. A., Grain boundary conduction of $Ce_{0.9}Gd_{0.1}O_{2-\delta}$ ceramics derived from oxalate coprecipitation: effects of Fe loading and sintering temperature. *Solid State Ionics*, 2005, **176**, 377–384.
29. Inada, H. and Tagawa, H., Ceria-based solid electrolytes. *Solid State Ionics*, 1996, **83**, 1–16.
30. Zheng, K., Steele, B. C. H., Saibzada, M. and Metcalfe, I. S., Solid state fuel cells on $Ce(Gd)O_{2-x}$ electrolytes. *Solid State Ionics*, 1996, **86–88**, 1241–1248.
31. Huang, K., Feng, M. and Goodenough, J. B., $Bi_2O_3$–$Y_2O_3$–$CeO_2$ solid solution oxide-ion electrolyte. *Solid State Ionics*, 1996, **89**, 17–24.
32. Zhang, T. S., Ma, J., Kong, L. B., Hing, P. and Kilner, J. A., Iron oxide as an effective aid and grain boundary scavenger for ceria-based electrolytes. *Solid State Ionics*, 2004, **167**, 203–207.